materials

MDPI

Article

Design of Strain-Hardening Natural TRM Composites: Current Challenges and Future Research Paths

Rogiros Illampas *, Daniel V. Oliveira and Paulo B. Lourenço

University of Minho, Institute for Sustainability and Innovation in Structural Engineering, Associate Laboratory Advanced Production and Intelligent Systems, Department of Civil Engineering, 4800-058 Guimarães, Portugal; danvco@civil.uminho.pt (D.V.O.); pbl@civil.uminho.pt (P.B.L.)

* Correspondence: d12925@civil.uminho.pt or rogiros@gmail.com

Abstract: This paper discusses the challenges in using natural fibers for the development of textile-reinforced mortar (TRM) composites with pseudo-strain-hardening and multiple cracking behavior. The particular characteristics of natural vegetal fibers are analyzed with reference to data from the literature. It is concluded that the efficient use of these fibers as composite reinforcement requires the development of treatment or impregnation protocols for overcoming durability issues, eliminating crimping effects in tensile response and imparting dimensional stability. Relevant experimental research on the synthesis and performance of natural TRMs is reviewed, showing that the fabrication of such systems is, at present, largely based on empirical rather than engineering design. In order to set a framework regarding the properties that the constituents of natural TRM must meet, a comparative analysis is performed against inorganic matrix composites comprising synthetic, mineral and metallic reinforcement. This highlights the need for selecting matrix materials compatible with natural fibers in terms of stiffness and strength. Furthermore, a rational methodology for the theoretical design of natural TRM composites is proposed. First-order analysis tools based on rule-of-mixtures and fracture mechanics concepts are considered. Based on the findings of this study, paths for future research are discussed.

Keywords: natural fibers; textile-reinforced mortar (TRM); composite materials; tensile response

Citation: Illampas, R.; Oliveira, D.V.; Lourenço, P.B. Design of Strain-Hardening Natural TRM Composites: Current Challenges and Future Research Paths. *Materials* **2023**, *16*, 4558. https://doi.org/10.3390/ma16134558

Academic Editor: Karim Benzarti

Received: 26 April 2023
Revised: 14 June 2023
Accepted: 16 June 2023
Published: 24 June 2023

1. Introduction

Textile-reinforced mortars (TRMs) are composite materials consisting of fiber textiles embedded in inorganic matrices (most commonly cement- or lime-based mortars). Such composites can be used as externally bonded reinforcement in the strengthening of existing buildings [1,2] or as structural materials for the construction of free-form structures and prefabricated components [3,4]. More recently, they have also been combined with thermal retrofitting systems for the concurrent structural and energy upgrading of buildings [5–7]. TRM systems offer several benefits, including a high strength-to-weight ratio, ease of application and minimal change in member geometry when used as strengthening layers. However, key challenges with respect to the sustainability and cost-efficiency of TRM solutions still need to be answered. The synthetic and mineral fiber textiles (e.g., glass, basalt, carbon) commonly used nowadays in TRM systems are costly and are produced using energy-intensive processes, and their end-of-life disposal entails a highly detrimental environmental impact. In addition, these types of textiles may not be suitable for the strengthening of relatively weak substrates such as historic masonry. This is because their high stiffness can cause premature cracking and/or slippage, precluding full exploitation of fiber strength. Natural fibers on the other hand are eco-friendly, renewable and have good economic feasibility. They also offer a higher degree of flexibility that precludes over-stiffening effects. In light of the above, researchers have been motivated to direct their efforts towards natural fiber inorganic matrix composites [8,9].

Despite the significant environmental and economic incentives that promote the development of natural TRM, there are several open issues in the engineering design of such systems. The mechanical behavior of textiles composed of natural fiber rovings differs significantly from that of textiles composed of man-made fibers. This is mainly due to the inferior strength and stiffness of natural fibers, the influence of crimping effects and the high variability in fiber properties. Furthermore, natural fibers show a high affinity to water and limited durability when exposed to alkaline environments. Although the design of brittle matrix composites has been studied in depth in the past and robust engineering analysis tools have been established, their applicability in the case of natural TRM has not yet been adequately explored. Instead, research is, at present, largely based on laboratory experimentation and empirical methods.

This paper aims to provide a framework for the engineering design of natural TRM composites with pseudo-strain-hardening and multiple cracking behavior. In order to assist in obtaining a more in-depth understanding of the mechanics of natural TRM, data from the literature regarding the characteristics of natural fibers is provided, while the synthesis and performance of composites examined in various studies are reviewed. A comparative analysis is performed between the properties of the constituents used in natural- and synthetic-fiber TRMs, with reference to both laboratory-tested and commercial systems. This enables the expression of practical guidelines concerning the selection of suitable matrix materials for natural TRMs. Finally, mechanics theories behind the design of continuous aligned fiber composites are presented and a rational approach for the theoretical design of natural TRM composites is proposed. The findings of this study enable identifying the specific problems that must be solved for advancing to real-life applications of natural TRMs in engineering. In this respect, paths for future research are also discussed.

2. Natural Fiber Reinforcement

Reinforcement in natural TRM composites comprises yarns, which are usually formed by twisted bundles of fibers. Table 1 presents the mechanical properties of different types of vegetal fiber yarns obtained from the literature. The typical tensile behavior of untreated yarns is illustrated in Figure 1. The initial response is nonlinear and is characterized by low stiffness, which progressively increases. This phenomenon is associated with the straightening and realignment of the crimped twisted fibers along the loading axis [10]. After the realignment of the fibers, a linear region occurs in the stress–strain curve. This is followed by random damage of the fibers within the yarn until the tensile capacity is reached and the yarn ruptures.

Table 1. Tensile strength (σ_{fu}), elastic modulus (E_f) and tensile failure strain (ε_{fu}) of dry natural fiber yarns considered in different studies as reinforcement in composites.

Fiber	Condition	σ_{fu} (MPa)	E_f (GPa)	ε_{fu} (%)	References
Flax	Untreated	195–417	5.5–25	1.6–6.2	[11–17]
	Treated [WT]	200–375	8–11	2.0–3.5	[16,18]
	Impregnated [RC, PC, NC]	220–631	9–38	1.3–3.6	[15,18,19]
Hemp	Untreated	120–296	3–27	1.0–5.4	[14–16]
	Treated [WT]	150–350	4–12	2.0–3.0	[16,18]
	Impregnated [RC, NC]	460–545	21–51	0.95–2.30	[15,18]
Jute	Untreated	75–225	2.7–10	0.02–7.0	[13,14,20,21]
	Treated [WT, AT]	36–102	0.5–1.5	5.0–12.0	[21]
	Impregnated [PC]	88	4.5	2.3	[20]
Sisal	Untreated	96–323	1.8–8	0.05–4.9	[12,14–16,22]
	Treated [WT]	220–320	5.5–9	3.0–4.0	[16]
	Impregnated [RC]	92–350	3.7–9	2.1–2.5	[15,22]

Table 1. *Cont.*

Fiber	Condition	σ_{fu} (MPa)	E_f (GPa)	ε_{fu} (%)	References
Cotton	Untreated	53	0.5	10	[15]
	Impregnated [RC]	82–92	0.8–0.9	7–8	[15]
Coir	Untreated	51	0.3	0.16	[14]

RC = resin coating; PC = polymer coating; NC = nanocomposite coating; WT = washing treatment; AT = alkali treatment.

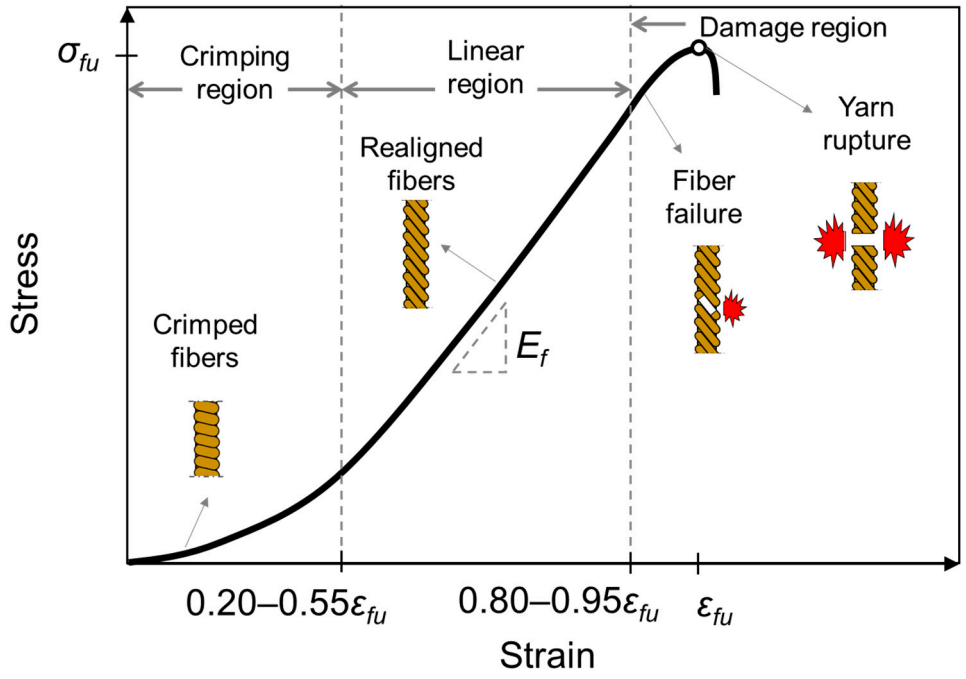

Figure 1. Typical stress–strain behavior of untreated natural fiber yarns under tension.

The inherent inhomogeneity and variable crimping status of twisted natural fibers result in significant dispersion in the mechanical properties of untreated yarns (see Table 1) and introduce uncertainties in the definition of TRM design parameters [23,24]. Very often, the crimping effect is ignored, and the yarns are regarded as linear elastic materials with elastic moduli equal to the slope of the linear part of the stress–strain curve. However, experimental results [11] show that untreated yarns may have to be stretched to >20% of their deformation capacity before the fibers are adequately strained so that linear behavior is attained. The strain at which crimping effects terminate may thus exceed by an order of magnitude the tensile cracking strain of common inorganic mortars. From an engineering design point of view, this means that upon cracking of the TRM matrix, the actual effective modulus of a reinforcing yarn would be much lower than the nominal value assumed.

In terms of physical properties, untreated yarns exhibit a high affinity to water due to the hydrophilicity of their constituent fibers. Cellulose-rich vegetal fibers tend to absorb water rapidly and sustain considerable dimensional changes upon variation in the moisture content [25,26]. This can adversely affect the fiber–matrix interface properties [27] and, hence, the end-performance of the TRM composite. Furthermore, natural fibers are prone to degradation inside alkaline cement- and lime-based mortars [28–31]. In such environments, degradation mechanisms associated with the mineralization of the fibers and deterioration of the lignin and hemicellulose occur, causing a reduction in the fibers' strength [11] and, subsequently, a decrease in the composite's toughness and cracking density [32].

To address the aforementioned drawbacks, several fiber treatments have been considered. These include a wide range of treatments for imparting hydrophobicity [33,34], washing protocols for cleansing the fibers' extractive content [16], and thermal and alkali

treatments for partially reducing non-cellulosic components such as hemicellulose, lignin, wax and impurities [35–37]. The removal of non-cellulosic impurities is believed to be the primary mechanism of strength enhancement in treated natural fibers [38–40]. After the removal of these materials, the interfibrillar region can become less dense and less rigid, allowing the fibrils to rearrange more easily along the direction of tensile deformation. Alkali treatments have also been found to improve chemical and mechanical anchoring to cementitious matrixes by exposing more reactive groups of cellulose to bond with the mortar paste and by increasing the fibers' surface roughness [40,41].

For increasing the initial stiffness and imparting a quasi-linear stress–strain response, the impregnation of yarns with polymers and resins has been considered [15,19,22]. Such coatings can penetrate the yarn structure, and as they harden and become more rigid, they create a surface layer with enhanced interlocking between the fibers thus producing a stiffening effect. Impregnated yarns behave as composites themselves, and their mechanical behavior is strongly influenced by the thickness of the coating layer [19]. In fact, relevant research has extended to the development of natural fiber-reinforced polymer bars that comprise multiple vegetal yarns impregnated in resin and are suitable for construction applications [42]. It should be noted that if the yarns are not adequately prestressed during the coating process, the twist and crimp of the fibers will remain upon impregnation and some reduction in the strength and deformation capacity will occur [43]. Furthermore, concerns are raised regarding the environmental impact of resin-based coatings. Recently, the use of tailored graphene/polyurethane nanocomposite coatings has been proposed [18]. This solution is promising as it can enhance the tensile properties and environmental resistance of yarns without compromising sustainability.

The natural textiles used in TRM fabrication typically have a woven structure with yarns arranged in the warp and weft directions forming a two-directional cross pattern (0°/90°). The tensile stress–strain behavior of untreated textiles is similar to that of individual yarns. Initially, the response is characterized by a nonlinear low stiffness zone due to decrimping and crimp interchange, while after the textile has been adequately stretched, the stiffness increases and the response becomes almost linear up to failure [44]. Composite element properties are influenced by the orientation and shape of the yarns within the textile [45]. Achieving higher reinforcing efficiency by controlling the alignment of the yarns so that these are straight and oriented in parallel with the loading direction can be challenging in natural TRMs. Untreated textiles have to be stretched for the yarns to remain straight during the fabrication process. Impregnation treatments can also result in dimensionally stable textiles. Certain coatings (e.g., resin-based impregnation), however, can cause over-stiffening and embrittlement, leading to damage to the textile when bent to fit on uneven surfaces. Furthermore, the impregnation of non-stretched yarns can lead to an irregular textile architecture. Stress development in the case of woven textiles is additionally affected by the yarns' crimping angle [46]. The influence is more pronounced in textiles with a high yarn density [47] where the closely bunched yarns exhibit large angles with respect to the loading direction. Finally, yarn spacing affects the constructability of TRMs since it controls the penetrability of the textile by the matrix.

3. Synthesis and Performance of Natural TRM Composites

For the fabrication of TRM composites, natural fibers are commonly embedded in cement- or lime-based mortars. Many studies [13–15,22,48–50] have considered the use of premixed commercial mortars that may contain, in addition to the primary binder and aggregate, different additives (e.g., pozzolanas, geopolymers) and admixtures (e.g., workability aids, synthetic resins). Mortars with fine granulometry (max. grain size < 2 mm) are generally preferred to ensure adequate penetrability within the textile grid. Much work has focused on natural TRMs comprising a hydraulic lime matrix. This is because the intended application is often the strengthening of heritage masonry structures, and this type of mortar is considered to be compatible with such substrates [51]. Laboratory-developed cementitious mortars have also been used [52–54]. Certain researchers examined the addition of short discrete fibers

in lime matrices, aiming to improve the post-crack behavior of TRM [55], while others considered the partial replacement of cement with pozzolanas (e.g., metakaolin, nanoclay) to reduce alkalinity and limit the deterioration of natural fibers [56,57]. The results show that dispersed fibers produce a bridging effect, which can lead to composites with denser crack patterns. The beneficial effects of dispersed fibers have been also verified by studies on hybrid cementitious composites [58–60]. However, their incorporation in the mortar matrix tends to decrease workability in the fresh state, making the use of plasticizing admixtures necessary. Pozzolanic additions in cementitious mortars were proven to reduce the calcium hydroxide phase, which is responsible for the degradation of the fibers' cellulose. Nevertheless, in the case of untreated textiles, the degradation of other fiber components (primarily hemicellulose) cannot be prevented with this solution [56].

Pull-out tests [19] on flax yarns embedded in lime mortar show that debonding behavior is characterized by a linear response up to the maximum bond stress (adhesive bond phase), followed by a drop in the load resistance and a frictional phase with quasi-constant residual strength. In cases where some degree of mechanical bond exists (e.g., due to surface irregularities of the yarns), the peak load is preceded by a hardening branch. Table 2 gives the maximum bond stress values reported in the literature for natural fibers embedded in inorganic matrices. The results exhibit noticeable dispersion, being influenced by the fiber embedment length [61] and the high variability of the fibers' geometric properties, which affects the mechanical/frictional bond [62]. Higher pull-out loads have been recorded after hornification, alkaline, peeling and nano-silica treatments [40,53]. Data regarding the effect that different coatings pose on bond behavior are somehow contradictory. Certain researchers [19,63] report a reduction in bond strength after coating with XSBR (carboxylate styrene butadiene rubber) and bio-based (cellulose acetate, cassava starch, hydrophobic starch) polymers. They have mainly attributed this behavior to the creation of a weak polymeric layer between the yarns/fibers and the mortar and to the lower surface roughness of coated yarns/fibers. Other researchers who considered XSBR and resin-based coatings [40,64,65] observed an improved response. Their results show that the interaction between XSBR and cementitious materials due to Ca^{2+} ions can enhance chemical and physical bonding [65], leading in some cases to a polymer-matrix bond that is even stronger than the fiber-coating bond [64]. Opposing trends may presumably be due to the particular characteristics of the fiber, matrix and coating materials used in various studies and to differences in the coating processes applied. The results may have been further influenced by the testing parameters adopted, as variations occur in the specimen types (cylindrical, prismatic, plated), clamping mechanisms, loading rates and embedment lengths considered. It should be underlined that the actual anchoring mechanisms of woven textiles are more complex than those of individual yarns/fibers. This is because the former is affected by the crimped geometry of the yarns within the textile, the frictional resistance at the warp–weft interlaces and the possible restraining action imposed by the yarns perpendicular to the load direction [66].

Table 3 presents the tensile properties of natural TRM composites, along with the characteristics of their constituent materials. Despite their variability, the results demonstrate that higher mechanical properties can be achieved by increasing the volumetric ratio of textile reinforcement and/or by using fibers with superior properties. Interestingly, the fiber reinforcement ratio in existing studies is not treated as an aspect of engineering design but rather as an experimental variable that is empirically modified until satisfactory results are obtained.

Figure 2 compares stress–strain curves obtained from tensile tests on TRM composites fabricated with untreated and treated flax textiles. The initial response is elastic up to the development of the first crack in the matrix. Given that an adequate volume of fiber reinforcement is provided, the elastic stage is followed by a multiple cracking zone in which a decrease in the composite's stiffness is observed. After the complete development of the crack pattern, an almost linear hardening branch occurs up to failure. The response in the last stage is mainly governed by the properties of the textile and of the textile–matrix

bond. Failure is usually either by rupturing of the yarns or by slippage of the textile within the matrix (telescopic failure). In composites with untreated fibers, a dramatic reduction in stress capacity (>70%) is observed upon the formation of the first crack. Even though specimens can eventually exhibit multi-cracking and pseudo-strain-hardening, experimental data indicate that upon crack initiation the load resistance may fall below an acceptable service limit. This phenomenon is probably associated with the particularly low initial elastic modulus of untreated fibers and with poor bonding between the untreated fibers and the matrix. The use of polymer-coated yarns was found to limit the load drops occurring after matrix cracking. Further improvement was attained by adding discrete short fibers in the matrix to impart post-crack tensile resistance.

Table 2. Maximum bond stress values from pull-out tests on yarns and single fibers embedded in inorganic matrices.

References	Matrix	Fiber			Embedment Length (mm)	Maximum Bond Stress (MPa)
		Type	Treatment	d_f (mm)		
[19]	Hydraulic lime	Flax	Untreated	1.56	25	0.30–0.40
			Polymer coated	1.00	25	0.15–0.30
[64]	Hydraulic lime	Hemp	Untreated	1.30	10–40	1.0–2.2
			Polymer coated	1.48	10–40	1.6–3.3
			Resin coated	1.60	30	>2.0
[67]	Geopolymer	Hemp	Untreated	0.55	10–20	0.80
[63]	Cement	Sisal *	Untreated	0.20	20–40	0.15–0.19
			Biopolymer coated	0.23	20–40	0.10
[40]	Cement	Sisal *	Untreated	0.66	25	0.18
			Hornified	0.26	25	0.27
			Alkali treated	0.45	25	0.32
			Polymer coated	0.75	25	0.34
			Hornified + Polymer coated	0.85	25	0.31
[65]	Cement	Sisal *	Untreated	0.10	25	0.24
			Polymer coated	0.10	25	0.49
		Curauá *	Untreated	0.17	25	0.21
			Polymer coated	0.17	25	0.52
		Jute *	Untreated	0.07	25	0.39
			Polymer coated	0.07	25	0.78
[62,68]	Cement	Jute *	Untreated	0.27	5–10	0.25–0.40
			Hot water immersion	0.27	5–10	0.30–0.34

* Tests conducted on single fibers.

Table 3. Characteristics of matrix (compressive strength—$f_{m,c}$, tensile strength—σ_{mu}, elastic modulus—E_m) and natural fiber reinforcement (textile area density—ρ_s, tensile strength—σ_{fu}, elastic modulus—E_f) used in different studies and corresponding properties of the composite (volumetric ratio of fiber reinforcement—V_f, initial elastic modulus—E_{c1}, tensile strength—σ_{cu}, exploitation ratio of the fiber reinforcement's tensile strength—$\sigma_{cu}/V_f\,\sigma_{fu}$).

References	Matrix				Reinforcement				Composite Properties			
	Type	$f_{m,c}$ (Mpa)	σ_{mu} (Mpa)	E_m (Gpa)	Type	ρ_s (g/m^2)	σ_{fu} (Mpa)	E_f (Gpa)	V_f (%)	E_{c1} (Gpa)	σ_{cu} (Mpa)	$\sigma_{cu}/V_f\,\sigma_{fu}$
[13]	Lime	7.7	2.8 [FL]	3.4	Flax	215	213	10.1	1.11	n/a	0.91	38%
									0.67	0.96	0.39	27%
									1.48	0.43	1.23	39%
									1.67	n/a	1.49	42%
					Flax	300	378	14.4	1.44	2.59	2.56	47%
									0.86	n/a	1.92	59%
									1.92	2.04	3.48	48%
									2.16	1.45	4.43	54%
					Jute	183	196	10.3	0.52	2.57	0.33	32%
									0.70	1.52	0.46	33%
									0.79	0.91	0.58	38%

Table 3. *Cont.*

References	Matrix				Reinforcement				Composite Properties			
	Type	$f_{m,c}$ (Mpa)	σ_{mu} (Mpa)	E_m (Gpa)	Type	ρ_s (g/m^2)	σ_{fu} (Mpa)	E_f (Gpa)	V_f (%)	E_{c1} (Gpa)	σ_{cu} (Mpa)	σ_{cu}/V_f σ_{fu}
[15]	Cement	39.3	4.6	8.9	Hemp [RC]	750	521	38.7	1.26	0.28	6.98	100%
					Hemp [RC]	990	544	50.6	1.26	0.16	5.99	87%
					Flax [RC]	770	631	36.0	1.26	0.18	5.24	66%
					Flax [RC]	1070	517	38.0	1.26	0.13	5.53	85%
					Sisal [RC]	2170	111	4.9	7.85	1.33	7.38	85%
					Sisal [RC]	2500	92	3.8	7.85	0.71	3.38	47%
					Cotton [RC]	1890	92	0.93	5.65	0.34	5.42	100%
					Cotton [RC]	2150	82	0.88	5.65	0.40	5.25	100%
[12,49]	Lime	14.6	1.0	n/a	Flax	375	397	9.9	1.32	0.30	2.22	42%
									1.35	3.65	2.65	49%
									2.11	0.32	3.84	46%
									2.70	3.81	8.32	78%
									4.05	4.29	12.88	80%
					Sisal	388	323	8.1	1.58	3.81	2.78	54%
									1.82	0.25	2.37	40%
									2.91	0.35	3.87	41%
									3.16	4.30	7.55	74%
									4.73	4.21	10.64	70%
[17,48,55]	Lime	9.5	4.2	n/a	Flax	300	331	12.5	1.30	n/a	1.56	36%
									2.30	n/a	4.51	59%
					Flax [PC]	n/a	266	12.4	1.60	n/a	2.86	67%
									2.50	n/a	4.35	65%
	Lime [DF]	9.9	2.9	n/a	Flax [PC]	n/a	266	12.4	2.20	n/a	4.20	72%
	Lime	11.1	3.1 [FL]	n/a	Flax	n/a	354	9.36	2.04	n/a	4.16	58%
									2.55	n/a	5.07	56%
[22]	Lime	13.0	3.5 [FL]	n/a	Sisal [AT]	Yarns	240	7.9	1.39	n/a	2.00	60%
[14]	Lime	12.2	3.1 [FL]	n/a	Jute	255	102	4.5	n/a	n/a	n/a	25%
					Jute	1099	225	3.7	n/a	n/a	n/a	16%
					Hemp	454	164	4.6	n/a	n/a	n/a	20%
					Flax	388	198	5.9	n/a	n/a	n/a	29%

Superscripts: DF = contains discrete fibers; FL = flexural tensile strength; RC = resin coated; PC = polymer coated; AT = alkali treated. n/a = not available data

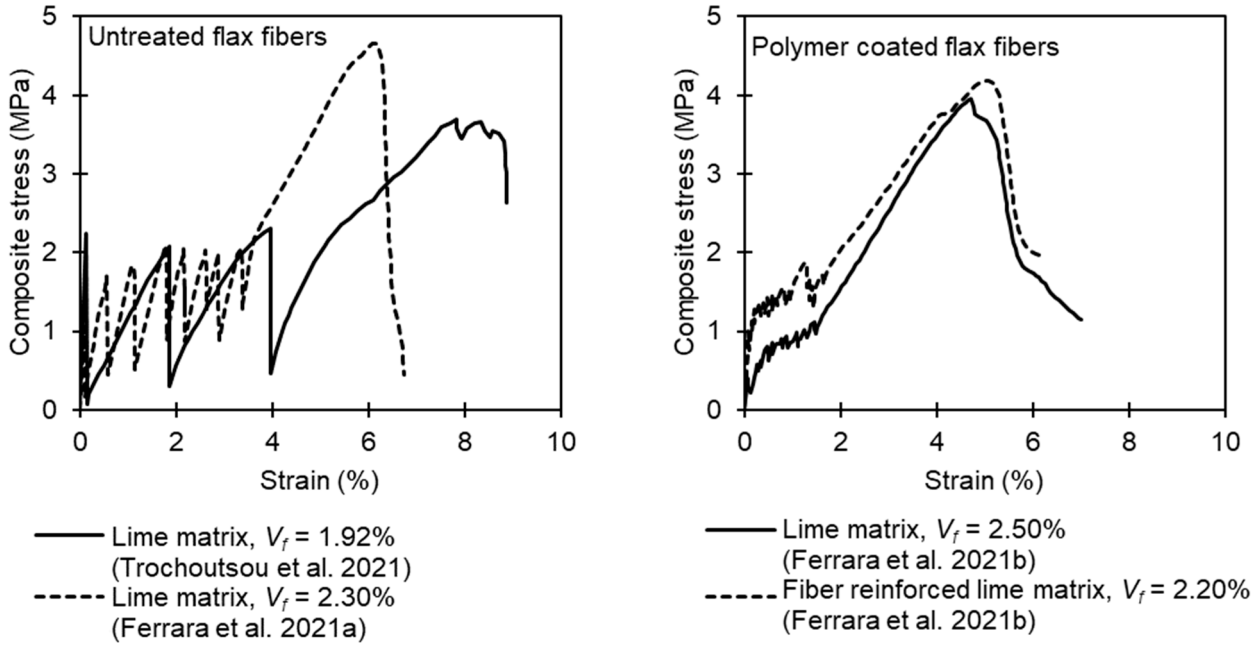

(**a**) (**b**)

Figure 2. Tensile stress–strain diagrams adapted by Trochoutsou et al. [13] and Ferrara et al. [48,55]: (**a**) untreated flax textiles embedded in hydraulic lime mortar; (**b**) polymer-coated flax textiles embedded in hydraulic lime mortar with and without dispersed short fibers.

A detailed review of the performance of natural TRM composites in strengthening applications can be found in Abbass et al. [69]. Promising results have been obtained in several studies considering natural TRM overlays on brick, stone and adobe masonry [17,70–76]. Overall, the experimental data show that such systems can potentially increase the bearing capacity and ductility of masonry elements under in-plane shear and eccentric axial loading and may also prevent brittle failure. The results obtained in certain studies [72,77], however, imply that the effectiveness of TRMs comprising untreated textiles can be hindered by slippage and/or delayed activation of the fiber reinforcement. The bonding of natural TRMs on masonry substrates has been found to be greatly influenced by the textile architecture and configuration [78]. The use of textiles with high yarn density and/or multiple textile plies can lead to poor matrix impregnation, thus promoting premature slippage and delamination phenomena.

4. Comparison between Natural TRM and Conventional Composite Systems

Inorganic matrix composites comprising synthetic (carbon, glass, polyparaphenylene benzobisoxazole (PBO)), mineral (basalt) and metallic (steel) reinforcement have been studied extensively in recent decades, both in the context of externally bonded strengthening applications and of thin element fabrication. Good practices regarding the composition of such systems have been established, and several commercialized systems have been developed. Given the background that exists on conventional composites, a comparative analysis is hereby presented aiming to define a framework concerning the characteristics that the constituents of natural TRM should meet. Table 4 summarizes data for basalt, carbon, glass, PBO and steel composites collected from twenty-five research studies [79–103] and from the specifications issued by twelve different material manufacturers (BASF, Biemme, CVR, Fassa Bartolo, FibreNet, G&P Intech, Kerakoll, Kimia, Mapei, Olympus, Ruregold, S&P, Sika) for 76 commercial systems. For each textile–matrix combination, the adopted reinforcing ratios (V_f) and the resulting tensile strength (expressed as a function of the reinforcement area σ_{cu}/V_f) and failure strain (ε_{cu}) of the composites are reported.

Table 4. Characteristics of textiles (tensile strength—σ_{fu}, elastic modulus—E_f) and matrices (compressive strength—$f_{m,c}$, flexural strength—$f_{m,fl}$, elastic modulus—E_m) used in conventional TRM systems.

Textile			**Matrix**				**Composite**		
Type	E_f **(GPa)**	σ_{fu} **(MPa)**	**Type(s)**	$f_{m,c}$ **(MPa)**	$f_{m,fl}$ **(MPa)**	E_m **(GPa)**	V_f **(%)**	σ_{cu}/V_f **(MPa)**	ε_{cu} **(%)**
Basalt	48–183	870–3080	Lime	11–21	3.2–6.3	4.9–15	0.1–0.8	357–1985	0.5–2.4
			Cement	21–45	2.5–12	8.2–20	0.3–1.4	1088–1256	1.9–2.2
Carbon	105–263	510–5000	Lime	10–18	3.2–6.7	8–16	0.4–2.1	369–2588	0.1–2.5
			Cement	20–119	3.5–12	7–39	0.3–5.2	422–3004	0.3–2.6
Glass	35–149	520–1850	Lime	10–21	2.2–9	5–16	0.2–2.4	255–2239	0.04–3.6
			Cement	15–79	3.5–9.9	7.6–34	0.1–7.2	172–1978	0.3–2.6
PBO	191–282	2470–3910	Lime	15	2	6	0.1–0.7	1817–2572	0.4–1.2
			Cement	20–80	2–9.3	6–39	0.1–0.6	1437–4670	0.2–2.0
Steel	130–210	1100–3210	Lime	13–21	3.2–5.5	9–15	0.06–2.6	2548–3364	1.2–2.2
			Cement	22–50	2.5–11.2	10–31.5	0.7–3.8	2231–3246	1.1–2.8
			Geopolymer	50–57	8–10.4	20–22.1	0.8–0.9	2231–2951	1.1–1.8

The mechanical properties of the matrix materials used in conventional systems typically satisfy certain performance criteria. Their compressive and flexural strengths are $f_{m,c}$ > 10 MPa and $f_{m,fl}$ > 2 MPa, respectively, to ensure adequate resistance against service loads. Their elastic modulus is generally an order of magnitude lower than that of the reinforcement to enable effective stress transfer to the fibers. The matrix type and composition mainly depend on the intended application. Lime-based matrices with $f_{m,c}$ = 10–15 MPa and $f_{m,fl}$ = 3–5 MPa are usually selected for systems to be applied on weak masonry sub-

strates. Cement or geopolymer mortars with $f_{m,c}$ = 25–60 MPa and $f_{m,fl}$ > 3.5 MPa are often preferred for strengthening concrete structures. High-strength ($f_{m,c}$ > 60 MPa) cementitious mixtures are mostly used for the fabrication of thin structural/architectural components.

Figure 3 compares the ratios between the elastic moduli of the reinforcement and matrices for various conventional composite systems. The range E_f/E_m reported for natural fibers is theoretical and was obtained assuming that E_f/E_m > 2 has to be adopted and that E_f/E_m cannot exceed 12.5 since natural fibers exhibit a maximum E_f in the range of 50 GPa, while a reasonable minimum value for E_m is 4 GPa. Data show that the ratio E_f/E_m, which affects composite response at the pre-crack and crack formation stages, can vary between 2 and 38 for conventional systems. In most cases, ratios E_f/E_m = 5–15 are found.

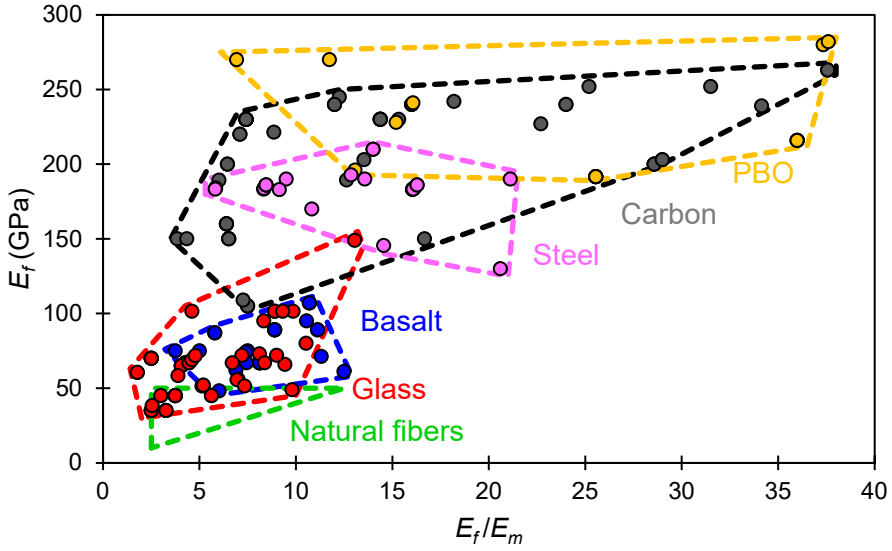

Figure 3. Elastic moduli of different reinforcement materials (E_f) used in continuous fiber composite systems and respective ratios between the elastic moduli of composites' reinforcement and matrix (E_f/E_m).

Although synthetic, mineral and metallic fibers exhibit superior mechanical properties than vegetal ones, their high tensile capacity (>500 MPa) cannot always be exploited (see, for example, data for basalt and carbon textiles in Table 4). This is particularly true in strengthening applications where fiber strength utilization is influenced by the textile-to-matrix and matrix-to-substrate bond. Tests conducted on TRM composites applied on brick masonry substrates [89,104] have shown that the bond strength at the interfaces quite often is far lower than the tensile capacity of high-strength fibers (i.e., steel and PBO). This gives rise to debonding phenomena associated with cohesive failure of the substrate or failure along the matrix-to-substrate or textile-to-matrix interfaces. A comparative study [75] examining the performance of PBO and flax TRM systems also concluded that the use of high-strength synthetic fibers on weak masonry substrates is inadvisable as debonding is likely to precede textile failure, thus precluding full exploitation of the reinforcement's tensile capacity. A more ductile bond-slip response with a higher fiber strength exploitation ratio was observed for flax TRM systems, indicating that these are more compatible with masonry. Nevertheless, the relatively lower strength of natural textiles can be a limiting factor in concrete strengthening applications. Flexural tests performed on concrete beams showed that synthetic textiles can significantly increase the members' post-yield moment capacity, despite the fact that the strengthening action can still be influenced by debonding and slippage phenomena [105,106]. Analogous experiments conducted using hemp TRM systems revealed that the tensile capacity of natural textiles can be reached at load levels near the member's yielding point, thus restricting strengthening action to the ultimate service limit state [107]. In terms of stiffness, natural textiles are only comparable with certain types of glass and basalt textiles that have elastic moduli

of 35–60 GPa. All other textile reinforcements used in conventional TRM systems have systematically higher elastic moduli.

Based on the above, it can be argued that matrices used in natural TRM should be tailored to give a ratio $E_f/E_m > 2$, while satisfying a threshold-bearing capacity $f_{m,c} > 6$ MPa. Matrix materials with elastic moduli in the range 4–10 GPa are likely to be suitable for textiles composed of coated flax and hemp yarns with elastic moduli of 10–50 GPa. This points towards the use of lime-based or low-strength cement mortars. Meeting the aforementioned criteria in the case of low-stiffness natural textiles can be difficult in practice. This is because modifying the mortar's mix design to substantially reduce the elastic modulus will most probably have an adverse effect on the material's bearing capacity. In this respect, achieving an acceptable E_f/E_m ratio without compromising strength is possibly unrealistic for jute, sisal, coir and cotton textiles with elastic moduli < 10 GPa.

5. Engineering Design of Natural TRM Composites

In the following, some basic considerations for the design of natural TRM composites with strain hardening and multi-cracking behavior are discussed. The analytical models hereafter proposed are mostly based on the well-established theories formulated by Aveston, Cooper and Kelly [108]. These researchers have used rule-of-mixtures and fracture mechanics concepts to describe the behavior of composite materials. The following basic assumptions have been made:

- The tensile response of both the matrix and the fibers is linear elastic–perfectly brittle and is characterized by (deterministic) fixed values of elastic modulus (E_m and E_f), tensile strength (σ_{mu} and σ_{fu}) and failure strain (ε_{mu} and ε_{fu}).
- The fibers are aligned parallel to one another and are uniformly distributed throughout the matrix.
- Forces are applied parallel to the fiber direction (i.e., the fiber reinforcement carries load only along the loading axis).
- The matrix is free of voids and the quantity of the fiber reinforcement (V_f) does not pose any influence on the porosity of the matrix, so the volumetric proportions of the two constituents are related as $V_m = 1 - V_f$.
- The composite is initially in a stress-free state, and there are no residual stresses arising from shrinkage phenomena, thermal expansion–contraction, etc.
- Poisson effects can be neglected.
- In the pre-crack state, there is perfect bonding between the fibers and the matrix, and hence, the strains on the fiber and matrix are equal, while the stresses are proportional to each constituent's elastic modulus.
- After a crack develops in the matrix and reaches the fibers, debonding at the fiber–matrix interface will occur.
- After debonding, stress transfer at the fiber–matrix interface is governed by friction only with a constant frictional bond shear strength (τ_s). It should be underlined that τ_s has no physical significance; it is merely a fictitious averaged bond shear strength that enables treating the complex stress-transfer problem in the context of practice-oriented design. It is also emphasized that the value of τ_s should not the confused with the maximum bond stress reported in Table 2.

Further details regarding the assumptions made when using the rule-of-mixtures for the calculation of the mechanical properties of composites prior to crack formation can be found in [109,110].

5.1. Critical Fiber Volume to Control Stress Transfer upon Cracking

In natural TRM composites where the failure strain of the matrix is typically much lower than the failure strain of the fibers ($\varepsilon_{mu} << \varepsilon_{fu}$), the first crack occurs when the tensile capacity of the matrix (σ_{mu}) is reached. Based on the assumption of elastic stress

distribution up to crack formation, the composite stress at the first crack (σ_{c1}) is given by [111]:

$$\sigma_{c1} = \sigma_{mu}\, V_m + \sigma'_f\, V_f \tag{1}$$

where σ'_f is the tensile stress of the fibers, which can be estimated as $\sigma'_f = E_f\, \varepsilon_{mu} = \sigma_{mu}\, (E_f/E_m)$ from strain compatibility.

After cracking of the matrix, the load will be thrown onto the fibers. If failure is to be prevented at this stage, the load-carrying capacity of the fiber reinforcement must be greater than the load on the composite at first crack [112], i.e., $\sigma_{fu}\, V_f \geq \sigma_{c1}$. The critical fiber volume can thus be calculated as:

$$V_{f,crit} \geq \frac{\sigma_{mu}}{\sigma_{fu} + \sigma_{mu}\left(1 - \frac{E_f}{E_m}\right)} \tag{2}$$

5.2. Critical Fiber Volume to Control Crack Spacing

The volumetric ratio of fiber reinforcement should be adequate to ensure that the crack spacing achieved is short enough for multiple cracks to develop along the specimen's length. The debonding length x_o, which is the distance from a crack face at which the matrix stress reaches its tensile capacity, is obtained from equilibrium (Figure 4):

$$x_o = \frac{\sigma_{mu} d_f V_m}{4\tau_s V_f} \tag{3}$$

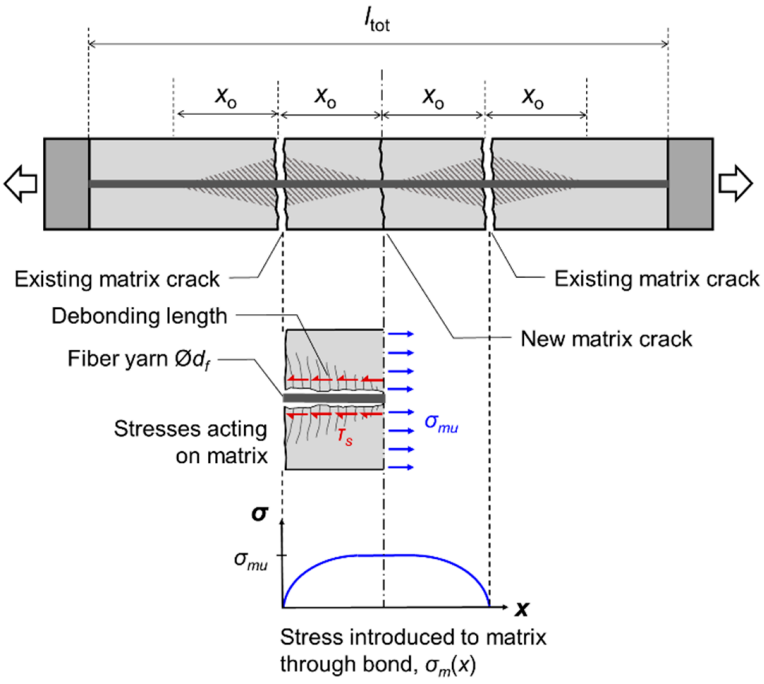

Figure 4. Distribution of stresses acting on the matrix between two cracks.

For $i \geq 2$ number of cracks to develop in a composite specimen ($i = 2$ cracks being the minimum condition for multi-cracking), the sum of the debonding lengths on either side of each crack should be lower than the total specimen length, i.e., $2ix_o \geq l_{tot}$. Based on the above, the critical fiber volume to control crack spacing is:

$$V_{f,crit} \geq \frac{i\sigma_{mu} d_f}{i\sigma_{mu} d_f + 2l_{tot}\tau_s} \tag{4}$$

Evidently, Equation (4) has some practical significance in the design of tensile specimens of limited length ($l_{tot} < 500$ mm). In actual TRM applications where the lengths of

composite layers are sufficiently large (typically in the order of meters), adequate frictional resistance can theoretically develop along the fiber–matrix interface to enable the formation of multiple cracks and to allow mobilization of the fiber strength.

5.3. Critical Fiber Volume to Limit the Drop in Load Resistance upon Formation of the First Crack

Under deformation-controlled tensile loading, the formation of the first crack is accompanied by a drop in load resistance. As the fibers bridge the crack, the load resistance increases again up to the formation of the next crack. Then, the load drops and increases again, and this is repeated until a crack saturation state is reached. Notably, the load drops observed in some studies examining natural TRM composites [13,48,49] are as high as 80% (see Figure 2). Therefore, the fiber volume provided should ensure sufficient residual strength after the formation of the first crack.

The method hereby proposed for estimating the fiber volume required to limit the drop in load resistance upon formation of the first crack is based on the model by Saidi and Gabor [95]. The latter assumes that the drop in load resistance depends on the reduction in the stiffness of the cracked specimen (i.e., on the global elastic modulus of the cracked composite). The cracked stiffness is a function of the specimen length, the volumetric ratios and elastic moduli of the matrix and fibers, and the debonding length. A schematic representation of the adopted model is given in Figure 5.

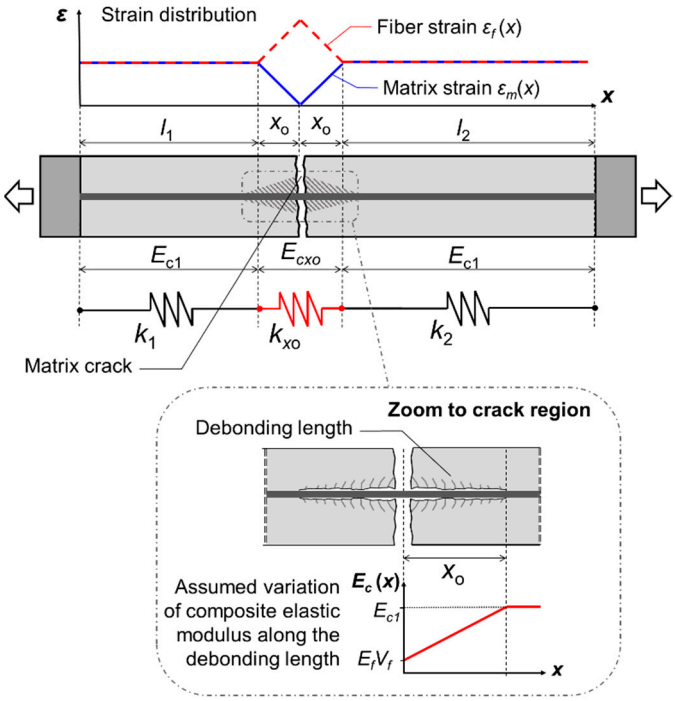

Figure 5. Schematic representation of the model used for determining the equivalent stiffness of the composite after the formation of the first matrix crack. The cracked stiffness is used for calculating the drop in load resistance upon cracking.

In the pre-cracking zone, the response of the composite is assumed to be elastic, and the initial elastic modulus (E_{c1}) is obtained from the rule of mixtures:

$$E_{c1} = E_m V_m + E_f V_f \quad (5)$$

After the formation of the first crack, the composite comprises three parts:

- A section that extends on both sides of the crack by a load transfer length x_o, over which debonding occurs. The local elastic modulus along the debonded interface (E_{cxo}) will be lower than the initial elastic modulus of the composite (E_{c1}). The part with a total length of $2x_o$ is characterized by a stiffness of k_{xo}.

- Two sections over which the fibers are fully bonded to the matrix and strain compatibility remains. The local elastic modulus along these two sections is equal to the initial elastic modulus of the composite (E_{c1}). The two sections have lengths l_1 and l_2 and their equivalent stiffnesses are k_1 and k_2.

The three parts can be considered as springs connected in a series. For a specimen with cross-sectional area A_c and total length $l_{tot} = l_1 + l_2 + 2x_o$, the global equivalent stiffness after the formation of the first crack (k_{eq}) is given by:

$$\frac{1}{k_{eq}} = \frac{l_{tot}}{A_c E_{c2}} = \frac{1}{k_1} + \frac{1}{k_2} + \frac{1}{k_{xo}} = \frac{l_1}{A_c E_{c1}} + \frac{l_2}{A_c E_{c1}} + \frac{2x_o}{A_c E_{cxo}} \tag{6}$$

In the above equation, E_{c2} is the global elastic modulus of the composite after the formation of the first crack.

For estimating the local elastic modulus of the composite over the length x_o, it is considered that the matrix does not contribute to the stiffness at the crack plane. At this position, the elastic modulus reduces to the equivalent modulus of the fiber reinforcement alone ($E_f V_f$). Moving away from the crack position, the matrix strain and the contribution of the matrix to the stiffness are assumed to increase and the elastic modulus reaches the nominal value E_{c1} at x_o. The evolution of the composite's elastic modulus along the debonding length ($0 \leq x \leq x_o$) is assumed to be linear and can be described by the equation:

$$E_c(x) = \frac{E_m V_m}{x_o} x + E_f V_f \tag{7}$$

The equivalent stiffness along the debonding length can be calculated considering this section as an assembly of infinitesimal elements of length dx connected in a series:

$$\frac{1}{k_{xo}} = \frac{x_o}{A_c E_{cxo}} = \int_0^{x_o} \frac{dx}{A_c E_c(x)} \tag{8}$$

Using Equations (7) and (8), the following expression is derived for the local elastic modulus over the debonding length:

$$E_{cxo} = \frac{E_m V_m}{\ln\left(\frac{E_{c1}}{E_f V_f}\right)} \tag{9}$$

The global elastic modulus of the composite specimen after the formation of the first crack (E_{c2}) is obtained by:

$$E_{c2} = \frac{l_{tot} E_{c1} E_{cxo}}{2x_o E_{c1} + E_{cxo}(l_{tot} - 2x_o)} \tag{10}$$

By assuming that crack propagation is instantaneous so that the global strain in the specimen just before and just after the formation of the first crack is the same, the stress drop (σ_{cdrop}) upon cracking can be attributed to a reduction in the global elastic modulus:

$$\varepsilon_{c1} = \frac{\sigma_{c1}}{E_{c1}} = \frac{\sigma_{c1} - \sigma_{cdrop}}{E_{c2}} \tag{11}$$

From Equation (11) the reduction in the load resistance of the composite is estimated as:

$$\frac{\sigma_{cdrop}}{\sigma_{c1}} = 1 - \frac{E_{c2}}{E_{c1}} \tag{12}$$

The critical fiber volume for limiting the drop in load resistance upon cracking ($V_{f,crit}$) is obtained using Equations (5), (9), (10) and (12) by setting an acceptable limit for the ratio $\sigma_{cdrop}/\sigma_{c1}$.

5.4. Control of Energy Absorption during Multiple Fracture

Using fracture mechanics concepts, it can be shown that fiber reinforcement can cause crack suppression in the matrix. In principle, cracking under tensile loading will occur when the failure strain of the matrix (ε_{mu}) is reached and provided also that there is a decrease in the potential energy of the composite specimen and the loading system. Considering the energy changes taking place when a crack is formed under conditions of fixed load (work performed by the applied stress, loss of strain energy in the matrix, increase in the fiber strain energy, work performed by frictional forces due to relative movement of the fibers in the matrix) and assuming a pure frictional fiber–matrix bond, Aveston, Cooper and Kelly [108] showed that if the fracture surface work in forming a crack in the matrix is γ_m, then a crack in the composite will only form if:

$$2\gamma_m V_m \leq \frac{E_c E_f \varepsilon_{mu}^3 \left(\frac{E_m V_m}{E_f V_f}\right)^2 d_f}{12\tau_s} \tag{13}$$

From Equation (13), it can be deduced that there is an upper limit of fiber content above which cracking will not occur at the normal failure strain of the matrix ε_{mu}, but the composite cracking strain will have to be increased to a strain ε_{muc} that is given by:

$$\varepsilon_{muc} = \left(\frac{24\tau_s \gamma_m E_f V_f^2}{E_c E_m^2 d_f V_m}\right)^{1/3} \tag{14}$$

Crack suppression in the matrix and multiple fracture will occur as long as the increased cracking stress (σ'_{c1}) does not exceed the capacity of the fiber reinforcement:

$$\sigma'_{c1} = E_c \varepsilon_{muc} < \sigma_{fu} V_f \tag{15}$$

In cases where the selected fiber content is high enough to result in increased cracking strain, the validity of Equation (15) should be verified as this marks the transition from multiple to single fracture.

5.5. Prediction of Tensile Stress–Strain Response

Figure 6 shows the Aveston–Cooper–Kelly (ACK) model describing the tensile stress–strain behavior of strain-hardening unidirectional composites. The model gives a simplified trilinear representation of the response under tension. The following three stages are identified:

- Stage I: The matrix is uncracked and a perfect bond between matrix and fabric is assumed. The elastic modulus of the uncracked composite is obtained by the rule of mixtures as per Equation (5). Stage I ends when the first crack occurs. The composite stress at the first crack can be calculated from Equation (1) or Equation (15), depending on whether the amount of fiber reinforcement can cause crack suppression in the matrix or not.
- Stage II: Provided that the fiber content is adequately high (see Section 5.1), the matrix material will exhibit multiple cracking until it reaches a crack stabilization (i.e., crack saturation) state. The ACK model assumes that the multiple cracking process continues at constant composite stress. Assuming that, in the post-crack state, a constant frictional shear stress develops along the debonded length x_o, the crack stabilization state is reached at a composite strain:

$$\varepsilon_{cs} = \left(1 + a\frac{E_m V_m}{E_f V_f}\right)\varepsilon_{mu} \tag{16}$$

Parameter a takes values between $\frac{1}{2}$ and $\frac{3}{4}$ and is commonly taken as $a = 0.666$ based on a theoretical average crack saturation spacing of $1.337x_o$ [113,114].

- Stage III: Additional loading after the crack stabilization stage will cause the fibers to stretch up to failure. Hence, the ultimate tensile strength of the composite (σ_{cu}) can be taken as equal to the tensile capacity of the embedded fiber reinforcement:

$$\sigma_{cu} = \sigma_{fu} V_f \quad (17)$$

Assuming that the modulus of elasticity in the post-multiple cracking zone is $E_f V_f$ (i.e., there is no contribution of the matrix to the global stiffness), the ultimate failure strain of the composite (ε_{cu}) will depend on the ultimate strain of the fiber and the crack spacing:

$$\varepsilon_{cu} = \varepsilon_{fu} - \varepsilon_{mu} \frac{E_m V_m}{E_f V_f} (1 - a) \quad (18)$$

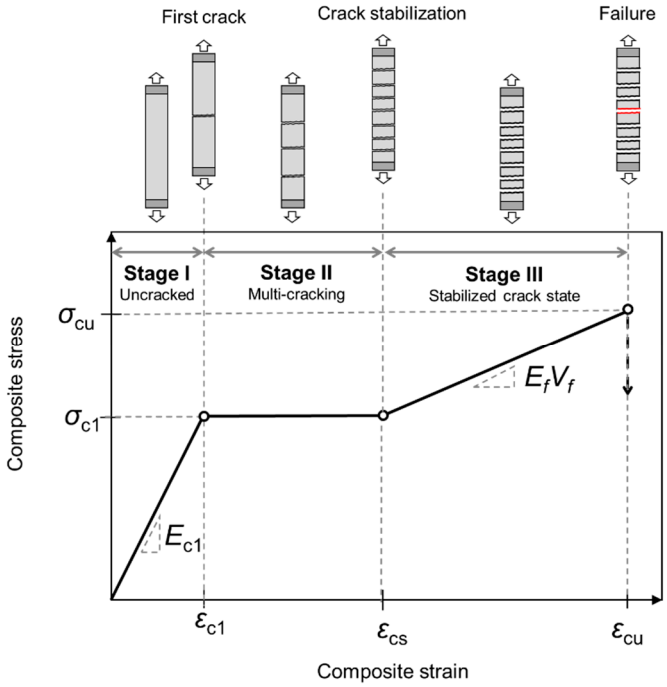

Figure 6. Trilinear representation of the tensile stress–strain response of a strain-hardening unidirectional composite according to the ACK model.

5.6. Design Example

The proposed methodology for calculating the required fiber reinforcement is hereby presented through a theoretical example. A hydraulic lime mortar with an elastic modulus of E_m = 9.5 GPa and a flexural strength of $f_{m,fl}$ = 3.5 MPa is considered as the matrix material. The uniaxial tensile strength of the matrix is approximated from the flexural strength considering a typical mortar specimen with depth h_b = 40 mm; $\sigma_{mu} = f_{m,fl}$ [$0.06 h_b{}^{0.7}$/(1 + $0.06 h_b{}^{0.7}$)] = 1.5 MPa [115]. The fracture energy of the matrix is taken as G_m = 26.3 N/m, which gives a surface energy of $\gamma_m = G_m/2$ = 13.15 N/m. The fiber reinforcement consists of hemp yarns with a tensile strength of σ_{fu} = 250 MPa and a nominal diameter of d_f = 1 mm. Two cases are examined: the use of treated fibers with an elastic modulus of E_f = 20 GPa, and the use of untreated fibers with an elastic modulus of E_f = 4 GPa. A composite tensile specimen with a free length of l_{tot} = 350 mm is assumed. The allowable drop in load resistance after the formation of the first crack is taken as $\sigma_{cdrop}/\sigma_{c1}$ = 20%.

Figure 7 presents the minimum volumetric proportions of fiber reinforcement required to achieve strain-hardening behavior with controlled crack spacing and adequate residual strength upon crack initiation. It also shows the quantity of fiber reinforcement above which crack suppression in the matrix will occur. The results are reported as a function of the fiber–matrix bond shear strength τ_s. The latter is assumed to take values from 0.1 up to

2 times σ_{mu}. It is indicatively noted that Eurocode 2 [116] recommends ratios τ_s/σ_{mu} in the range 0.9 to 1.9 to describe the shear resistance of the interface between concrete and steel reinforcement (the lower ratio refers to bars with an effectively plain surface and the higher ratio refers to high-bond ribbed bars).

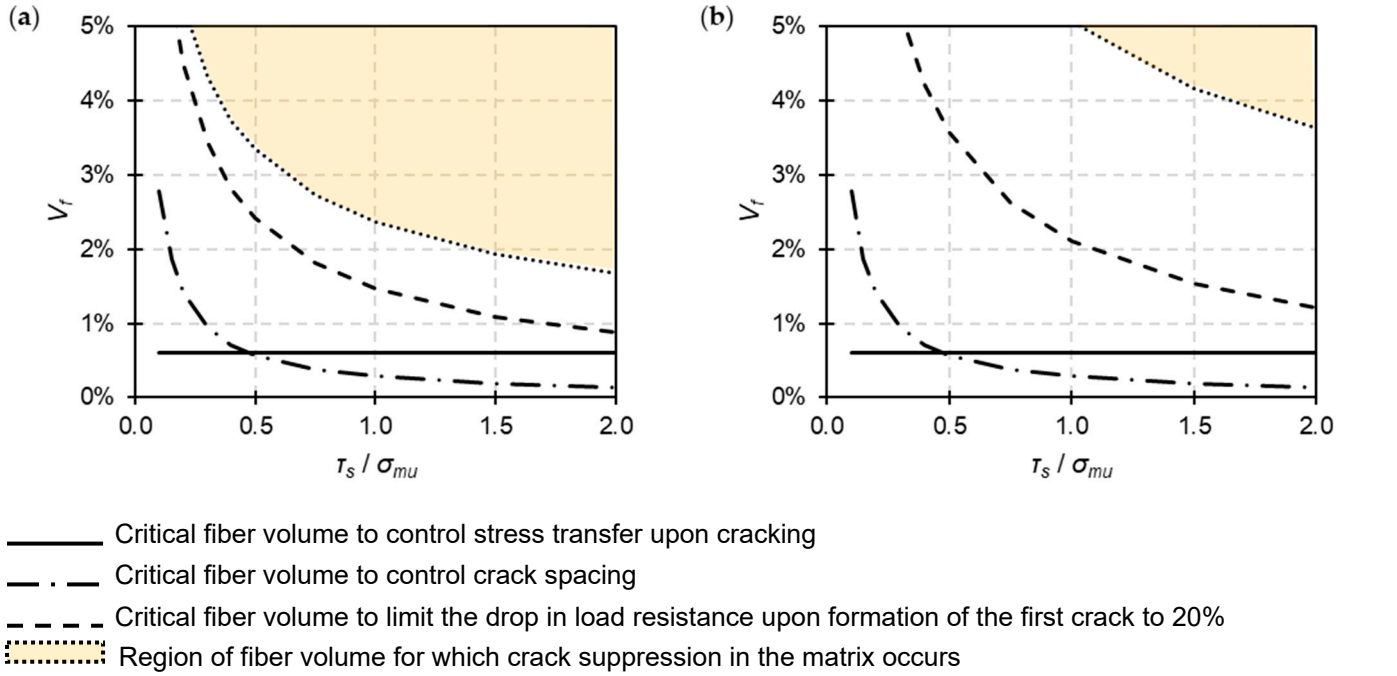

Figure 7. Fiber volumes required to control stress transfer upon cracking, crack spacing, residual resistance upon crack formation and crack suppression in the matrix as a function of the ratio between the fiber–matrix frictional bond shear strength and the matrix tensile strength. (**a**) Treated fibers with E_f = 20 GPa and (**b**) untreated fibers with E_f = 4 GPa.

According to the analysis, $V_f > 0.61\%$ is, in both cases, adequate to prevent failure of the composite after the matrix cracks. For $\tau_s/\sigma_{mu} < 0.5$, the volume of fiber reinforcement required to control crack spacing becomes higher than that required to avoid failure after cracking. Nevertheless, for the entire range of τ_s/σ_{mu} ratios considered, it was found that a substantially higher volume of fiber reinforcement is required to limit the drop in load resistance upon crack formation. This is particularly true for low-modulus untreated fibers, where achieving $\sigma_{cdrop}/\sigma_{c1} \leq 20\%$ entails a more than twofold increase in the critical fiber volume computed from Equation (2). In fact, for $\tau_s/\sigma_{mu} < 0.5$, the volume of untreated fibers required to achieve adequate residual capacity upon cracking is $V_f > 3.5\%$. Therefore, it can be argued that poor shear bond strength is to a large degree responsible for the high drops in load resistance that were observed in certain studies (see Figure 2a), despite the use of rather high fiber volumes ($V_f \sim 2\%$). The calculations also show that crack suppression in the matrix is not likely to occur with the type of untreated fiber hereby considered, as the volumetric ratios of reinforcement required to impart such behavior are unrealistically high, even for a good fiber–matrix bond ($V_f > 3.6\%$ for $\tau_s/\sigma_{mu} = 2$).

The design example also introduces some interesting constructability aspects. When $\tau_s/\sigma_{mu} < 1.4$, the demand in untreated fiber reinforcement becomes $V_f > 1.6\%$. This means that for the construction of a typical 10 mm-thick TRM overlay, a hemp textile with mesh spacing < 5 mm should be used. Such low mesh spacing is impractical as it will impede effective penetration from the mortar matrix. Hence, multiple plies of textile will have to be used. Using treated fibers, a single-ply TRM with $V_f < 1.6\%$ can be realized when $\tau_s/\sigma_{mu} > 0.8$.

Overall, the results highlight the influence that the fiber–matrix interface properties have on the response of the composite. Adequately high bond resistance is necessary to

achieve multi-cracking behavior and to prevent the load resistance from dropping below an acceptable serviceability limit upon matrix cracking, while reasonably limiting the volumetric ratio of fiber reinforcement. It should be emphasized, however, that excessively high interfacial bond strength can lead to premature fiber rapture, precluding strain-hardening behavior. Further discussion on this issue can be found in Li and Wu [117], where a fracture mechanics approach is used to show that, for fixed fiber and matrix properties, there is an upper limit on the frictional bond strength.

6. Conclusions and Recommendations for Future Research

Natural fibers constitute a sustainable alternative to man-made fibers and have good potential for the fabrication of inorganic matrix composites used in construction. At this stage, however, the realization of natural TRM systems that can be safely adopted in real-life structural applications remains a challenging task, and further research is required. This paper highlighted critical issues that need to be addressed in this direction. Based on the analysis of the data presented, the following future research trends are identified:

- A framework for the rational engineering design of natural TRM composites should be formulated. This should become the theoretical basis of experimental campaigns dealing with natural composites. In this study, some of the classical mechanics and fracture mechanics theories for the analysis of continuous aligned fiber composites have been introduced. Such theories constitute a good starting point for the development of design tools tailored to natural TRM. More advanced computational models should also be explored. Design methods must account for the particular mechanical behavior of natural fibers and must be validated against experimental data.
- The development of suitable fiber treatments is essential for overcoming durability problems, for eliminating the initially nonlinear tensile response of crimped yarns and for imparting dimensional stability to textiles. In this respect, emphasis should be placed on coating protocols that can achieve the fiber mechanical response required for functional TRM systems. Particular reference is made to graphene/polyurethane nanocomposite coatings as these have better environmental merits than epoxy- and resin-based impregnation. Upscaling of coating methods from the laboratory to the industrial scale is also necessary for advancement to commercialized TRM systems.
- Matrix materials compatible with natural fibers should be developed. Mortars suited to natural TRM should have a low elastic modulus but should also possess an adequate bearing capacity to ensure good performance under service loads. Different additives and admixtures can be considered for improving the bond behavior and for reducing alkalinity to prevent fiber deterioration. Another research direction lies in the design of hybrid systems comprising textiles embedded in matrices reinforced with dispersed short fibers. The addition of discrete fibers in the TRM matrix is expected to enhance the composite's load-deformation and energy absorption characteristics, resulting in improved post-crack behavior. This solution can promote the use of natural fibers in the form of dispersed mortar reinforcement and can also limit the significant load drops that tend to occur upon the cracking of natural TRM.
- The fiber–matrix bond behavior should be studied in depth since the interface properties influence the end performance of the composite to a great extent. To this end, the development of TRM systems should include the implementation of pullout tests at different embedment lengths. Relevant experimental data will assist in the derivation of useful design parameters (e.g., the critical bond length beyond which fiber failure prevails over debonding, the value of the frictional bond strength, etc.) and may also be utilized in the context of more rigorous analysis for the derivation of bond-slip laws.
- Alternative typologies of composites should be examined in order to overcome constructability issues arising in cases where high quantities of fiber reinforcement are required. A possible solution lies in the design of composite-reinforced mortar (CRM) systems. Compared to TRM systems that comprise textiles with close yarn spacing, CRM systems comprise preformed meshes composed of impregnated fiber bars ar-

ranged in a relatively wide pitch. The development of such reinforcing systems can benefit from research on the fabrication of natural yarn bars.

Author Contributions: Conceptualization, R.I. and D.V.O.; methodology, R.I. and D.V.O.; validation, R.I., D.V.O. and P.B.L.; formal analysis, R.I., D.V.O. and P.B.L.; investigation, R.I.; resources, R.I., D.V.O. and P.B.L.; data curation, R.I.; writing—original draft preparation, R.I.; writing—review and editing, R.I., D.V.O. and P.B.L.; visualization, R.I. and D.V.O.; supervision, D.V.O. and P.B.L.; project administration, R.I., D.V.O. and P.B.L.; funding acquisition, R.I., D.V.O. and P.B.L. All authors have read and agreed to the published version of the manuscript.

Funding: This research has been funded by the European Union's Horizon 2020 research and innovation programme under the Marie Skłodowska-Curie grant agreement No 101038078. This work was partly financed by FCT/MCTES through national funds (PIDDAC) under the R&D Unit Institute for Sustainability and Innovation in Structural Engineering (ISISE), under reference UIDB/04029/2020, and under the Associate Laboratory Advanced Production and Intelligent Systems ARISE under reference LA/P/0112/2020.

Institutional Review Board Statement: Not applicable.

Informed Consent Statement: Not applicable.

Data Availability Statement: Not applicable.

Conflicts of Interest: The authors declare no conflict of interest. The funders had no role in the design of the study; in the collection, analyses, or interpretation of data; in the writing of the manuscript; or in the decision to publish the results.

Nomenclature

γ_m	Fracture surface work for forming a crack in the matrix
ε_{cs}	Composite strain at crack stabilization stage
ε_{cu}	Composite strain at failure
ε_{mu}	Failure strain of the matrix
ε_{fu}	Failure strain of the fiber
σ_{c1}	Composite stress corresponding to the formation of the first crack
σ_{cdrop}	Drop in composite stress after the formation of the first crack
σ_{cu}	Composite tensile failure stress
σ_{mu}	Tensile strength of the matrix
σ_{fu}	Tensile strength of the fiber
τ_s	Frictional bond strength
a	Factor for calculating the composite strain at the crack stabilization stage
d_f	Fiber diameter
E_{c1}	Initial elastic modulus of the composite
E_{c2}	Elastic modulus of the composite after the formation of the first crack
E_{cxo}	Elastic modulus of the composite along the debonded interface
E_m	Elastic modulus of the matrix
E_f	Elastic modulus of the fiber
$f_{m,c}$	Compressive strength of the matrix
$f_{m,fl}$	Flexural strength of the matrix
G_m	Matrix fracture energy
k_i	Equivalent stiffness of a composite zone with full fiber–matrix bond
k_{xo}	Equivalent stiffness of the composite along the debonding length
l_{tot}	Total length of specimen
l_i	Lengths of specimen sections with full matrix–fiber bond
x_o	Debonding length
V_f	Fiber volume
$V_{f,crit}$	Critical fiber volume
V_m	Matrix volume

References

1. Kouris, L.A.S.; Triantafillou, T.C. State-of-the-Art on Strengthening of Masonry Structures with Textile Reinforced Mortar (TRM). *Constr. Build. Mater.* **2018**, *188*, 1221–1233. [CrossRef]
2. Koutas, L.N.; Tetta, Z.; Bournas, D.A.; Triantafillou, T.C. Strengthening of Concrete Structures with Textile Reinforced Mortars: State-of-the-Art Review. *J. Compos. Constr.* **2019**, *23*, 03118001. [CrossRef]
3. Venigalla, S.G.; Nabilah, A.B.; Mohd Nasir, N.A.; Safiee, N.A.; Abd Aziz, F.N.A. Textile-Reinforced Concrete as a Structural Member: A Review. *Buildings* **2022**, *12*, 474. [CrossRef]
4. Papanicolaou, C.G. Applications of Textile-Reinforced Concrete in the Precast Industry. In *Textile Fibre Composites in Civil Engineering*; Elsevier: Amsterdam, The Netherlands, 2016; pp. 227–244. ISBN 978-1-78242-446-8.
5. Bournas, D.A. Concurrent Seismic and Energy Retrofitting of RC and Masonry Building Envelopes Using Inorganic Textile-Based Composites Combined with Insulation Materials: A New Concept. *Compos. Part B Eng.* **2018**, *148*, 166–179. [CrossRef]
6. Illampas, R.; Rigopoulos, I.; Ioannou, I. Influence of Microencapsulated Phase Change Materials (PCMs) on the Properties of Polymer Modified Cementitious Repair Mortar. *J. Build. Eng.* **2021**, *40*, 102328. [CrossRef]
7. Ademovic, N.; Formisano, A.; Penazzato, L.; Oliveira, D.V. Seismic and Energy Integrated Retrofit of Buildings: A Critical Review. *Front. Built Environ.* **2022**, *8*, 963337. [CrossRef]
8. Ali, M. Natural Fibres as Construction Materials. *J. Civ. Eng. Constr. Technol.* **2012**, *3*, 80–89. [CrossRef]
9. Laverde, V.; Marin, A.; Benjumea, J.M.; Rincón Ortiz, M. Use of Vegetable Fibers as Reinforcements in Cement-Matrix Composite Materials: A Review. *Constr. Build. Mater.* **2022**, *340*, 127729. [CrossRef]
10. Wang, J.; Zhou, H.; Liu, Z.; Peng, X.; Zhou, H. Statistical Modelling of Tensile Properties of Natural Fiber Yarns Considering Probability Distributions of Fiber Crimping and Effective Yarn Elastic Modulus. *Compos. Sci. Technol.* **2022**, *218*, 109142. [CrossRef]
11. Ferrara, G.; Coppola, B.; Di Maio, L.; Incarnato, L.; Martinelli, E. Tensile Strength of Flax Fabrics to Be Used as Reinforcement in Cement-Based Composites: Experimental Tests under Different Environmental Exposures. *Compos. Part B Eng.* **2019**, *168*, 511–523. [CrossRef]
12. Cevallos, O.A.; Olivito, R.S. Effects of Fabric Parameters on the Tensile Behaviour of Sustainable Cementitious Composites. *Compos. Part B Eng.* **2015**, *69*, 256–266. [CrossRef]
13. Trochoutsou, N.; Di Benedetti, M.; Pilakoutas, K.; Guadagnini, M. Mechanical Characterisation of Flax and Jute Textile-Reinforced Mortars. *Constr. Build. Mater.* **2021**, *271*, 121564. [CrossRef]
14. Codispoti, R.; Oliveira, D.V.; Olivito, R.S.; Lourenço, P.B.; Fangueiro, R. Mechanical Performance of Natural Fiber-Reinforced Composites for the Strengthening of Masonry. *Compos. Part B Eng.* **2015**, *77*, 74–83. [CrossRef]
15. Mercedes, L.; Gil, L.; Bernat-Maso, E. Mechanical Performance of Vegetal Fabric Reinforced Cementitious Matrix (FRCM) Composites. *Constr. Build. Mater.* **2018**, *175*, 161–173. [CrossRef]
16. Abbass, A.; Paiva, M.C.; Oliveira, D.V.; Lourenço, P.B.; Fangueiro, R. Insight into the Effects of Solvent Treatment of Natural Fibers Prior to Structural Composite Casting: Chemical, Physical and Mechanical Evaluation. *Fibers* **2021**, *9*, 54. [CrossRef]
17. Ferrara, G.; Caggegi, C.; Martinelli, E.; Gabor, A. Shear Capacity of Masonry Walls Externally Strengthened Using Flax-TRM Composite Systems: Experimental Tests and Comparative Assessment. *Constr. Build. Mater.* **2020**, *261*, 120490. [CrossRef]
18. Abbass, A.; Paiva, M.C.; Oliveira, D.V.; Lourenço, P.B.; Fangueiro, R. Graphene/Polyurethane Nanocomposite Coatings—Enhancing the Mechanical Properties and Environmental Resistance of Natural Fibers for Masonry Retrofitting. *Compos. Part Appl. Sci. Manuf.* **2023**, *166*, 107379. [CrossRef]
19. Ferrara, G.; Pepe, M.; Martinelli, E.; Dias Tolêdo Filho, R. Influence of an Impregnation Treatment on the Morphology and Mechanical Behaviour of Flax Yarns Embedded in Hydraulic Lime Mortar. *Fibers* **2019**, *7*, 30. [CrossRef]
20. Fidelis, M.E.A.; Toledo Filho, R.D.; de Silva, F.A.; Mechtcherine, V.; Butler, M.; Hempel, S. The Effect of Accelerated Aging on the Interface of Jute Textile Reinforced Concrete. *Cem. Concr. Compos.* **2016**, *74*, 7–15. [CrossRef]
21. Majumder, A.; Stochino, F.; Farina, I.; Valdes, M.; Fraternali, F.; Martinelli, E. Physical and Mechanical Characteristics of Raw Jute Fibers, Threads and Diatons. *Constr. Build. Mater.* **2022**, *326*, 126903. [CrossRef]
22. de Carvalho Bello, C.B.; Boem, I.; Cecchi, A.; Gattesco, N.; Oliveira, D.V. Experimental Tests for the Characterization of Sisal Fiber Reinforced Cementitious Matrix for Strengthening Masonry Structures. *Constr. Build. Mater.* **2019**, *219*, 44–55. [CrossRef]
23. Belaadi, A.; Bourchak, M.; Aouici, H. Mechanical Properties of Vegetal Yarn: Statistical Approach. *Compos. Part B Eng.* **2016**, *106*, 139–153. [CrossRef]
24. Akter, S.; Helali, M.M. The Effect of Mechanical Crimp on the Basic Properties of Jute Yarn. *Mater. Today Proc.* **2021**, *46*, 425–432. [CrossRef]
25. de Martel, W.N.D.R.; Salgado, I.P.; Silva, F.A. The Influence of Fiber Treatment on the Morphology, Water Absorption Capacity and Mechanical Behavior of Curauá Fibers. *J. Nat. Fibers* **2022**, *19*, 642–657. [CrossRef]
26. John, M.; Thomas, S. Biofibres and Biocomposites. *Carbohydr. Polym.* **2008**, *71*, 343–364. [CrossRef]
27. Zafeiropoulos, N.E. (Ed.) *Interface Engineering of Natural Fibre Composites for Maximum Performance*; Woodhead Publishing: Oxford, UK, 2016; ISBN 978-0-08-101742-5.
28. Ramakrishna, G.; Sundararajan, T. Studies on the Durability of Natural Fibres and the Effect of Corroded Fibres on the Strength of Mortar. *Cem. Concr. Compos.* **2005**, *27*, 575–582. [CrossRef]
29. Tolêdo Filho, R.D.; Scrivener, K.; England, G.L.; Ghavami, K. Durability of Alkali-Sensitive Sisal and Coconut Fibres in Cement Mortar Composites. *Cem. Concr. Compos.* **2000**, *22*, 127–143. [CrossRef]

30. de Carvalho Bello, C.B.; Cecchi, A.; Ferrara, L. Assessing the Alkali-Sensitivity of the Mechanical Behavior of Jute Fibers to Evaluate Their Durability in Cementitious Composites Applications. In Proceedings of the 3rd RILEM Spring Convention and Conference (RSCC 2020), Guimarães, Portugal, 9–14 March 2020; Valente, I.B., Ventura Gouveia, A., Dias, S.S., Eds.; RILEM Bookseries. Springer International Publishing: Cham, Switzerland, 2021; Volume 33, pp. 151–157.
31. de Bello, C.B.C.; Cecchi, A. Experiments on Natural Fibers: Durability and Mechanical Properties. *Adv. Mater. Process. Technol.* **2017**, *3*, 632–639. [CrossRef]
32. de Melo Filho, J.A.; Silva, F.d.A.; Toledo Filho, R.D. Degradation Kinetics and Aging Mechanisms on Sisal Fiber Cement Composite Systems. *Cem. Concr. Compos.* **2013**, *40*, 30–39. [CrossRef]
33. Ali, A.; Shaker, K.; Nawab, Y.; Jabbar, M.; Hussain, T.; Militky, J.; Baheti, V. Hydrophobic Treatment of Natural Fibers and Their Composites—A Review. *J. Ind. Text.* **2018**, *47*, 2153–2183. [CrossRef]
34. Abbass, A.; Paiva, M.C.; Oliveira, D.V.; Lourenço, P.B.; Fangueiro, R.; Alves, N.M. The Potential of Beeswax Colloidal Emulsion/Films for Hydrophobization of Natural Fibers Prior to NTRM Manufacturing. *Key Eng. Mater.* **2022**, *916*, 82–90. [CrossRef]
35. Wei, J.; Meyer, C. Improving Degradation Resistance of Sisal Fiber in Concrete through Fiber Surface Treatment. *Appl. Surf. Sci.* **2014**, *289*, 511–523. [CrossRef]
36. Le Troëdec, M.; Dalmay, P.; Patapy, C.; Peyratout, C.; Smith, A.; Chotard, T. Mechanical Properties of Hemp-Lime Reinforced Mortars: Influence of the Chemical Treatment of Fibers. *J. Compos. Mater.* **2011**, *45*, 2347–2357. [CrossRef]
37. Arsène, M.-A.; Okwo, A.; Bilba, K.; Soboyejo, A.B.O.; Soboyejo, W.O. Chemically and Thermally Treated Vegetable Fibers for Reinforcement of Cement-Based Composites. *Mater. Manuf. Process.* **2007**, *22*, 214–227. [CrossRef]
38. Gassan, J.; Bledzki, A.K. Alkali Treatment of Jute Fibers: Relationship between Structure and Mechanical Properties. *J. Appl. Polym. Sci.* **1999**, *71*, 623–629. [CrossRef]
39. Kundu, S.P.; Chakraborty, S.; Roy, A.; Adhikari, B.; Majumder, S.B. Chemically Modified Jute Fibre Reinforced Non-Pressure (NP) Concrete Pipes with Improved Mechanical Properties. *Constr. Build. Mater.* **2012**, *37*, 841–850. [CrossRef]
40. Ferreira, S.R.; de Silva, F.A.; Lima, P.R.L.; Toledo Filho, R.D. Effect of Fiber Treatments on the Sisal Fiber Properties and Fiber–Matrix Bond in Cement Based Systems. *Constr. Build. Mater.* **2015**, *101*, 730–740. [CrossRef]
41. Castoldi, R.D.S.; De Souza, L.M.S.; Souto, F.; Liebscher, M.; Mechtcherine, V.; De Andrade Silva, F. Effect of Alkali Treatment on Physical–Chemical Properties of Sisal Fibers and Adhesion towards Cement-Based Matrices. *Constr. Build. Mater.* **2022**, *345*, 128363. [CrossRef]
42. Sharkawi, A.M.; Mehriz, A.M.; Showaib, E.A.; Hassanin, A. Performance of Sustainable Natural Yarn Reinforced Polymer Bars for Construction Applications. *Constr. Build. Mater.* **2018**, *158*, 359–368. [CrossRef]
43. Ungerer, B.; Müller, U.; Pramreiter, M.; Herrero Acero, E.; Veigel, S. Influence of Yarn Structure and Coating on the Mechanical Performance of Continuous Viscose Fiber/Epoxy Composites. *Polym. Compos.* **2022**, *43*, 1012–1021. [CrossRef]
44. Misnon, M.I.; Islam, M.M.; Epaarachchi, J.A.; Lau, K.T. Analyses of Woven Hemp Fabric Characteristics for Composite Reinforcement. *Mater. Des. 1980–2015* **2015**, *66*, 82–92. [CrossRef]
45. Peled, A.; Mobasher, B.; Bentur, A. *Textile Reinforced Concrete*, 1st ed.; CRC Press: Boca Raton, FL, USA, 2017; ISBN 978-1-315-11915-1.
46. Peled, A.; Bentur, A. Geometrical Characteristics and Efficiency of Textile Fabrics for Reinforcing Cement Composites. *Cem. Concr. Res.* **2000**, *30*, 781–790. [CrossRef]
47. El Messiry, M.; Mito, A.-B.; Al-Oufy, A.; El-Tahan, E. Effect of Fabric Material and Tightness on the Mechanical Properties of Fabric–Cement Composites. *Alex. Eng. J.* **2014**, *53*, 795–801. [CrossRef]
48. Ferrara, G.; Pepe, M.; Martinelli, E.; Tolêdo Filho, R.D. Tensile Behavior of Flax Textile Reinforced Lime-Mortar: Influence of Reinforcement Amount and Textile Impregnation. *Cem. Concr. Compos.* **2021**, *119*, 103984. [CrossRef]
49. Olivito, R.S.; Cevallos, O.A.; Carrozzini, A. Development of Durable Cementitious Composites Using Sisal and Flax Fabrics for Reinforcement of Masonry Structures. *Mater. Des.* **2014**, *57*, 258–268. [CrossRef]
50. Ghiassi, B.; Razavizadeh, A.; Oliveira, D.V.; Marques, V.; Lourenço, P.B. Tensile and Bond Characterization of Natural Fibers Embeeded in Inorganic Matrices. In *Natural Fibres: Advances in Science and Technology Towards Industrial Applications*; Fangueiro, R., Rana, S., Eds.; RILEM Bookseries; Springer: Dordrecht, The Netherlands, 2016; Volume 12, pp. 305–314. ISBN 978-94-017-7513-7.
51. Ghiassi, B. Mechanics and Durability of Lime-Based Textile Reinforced Mortars. *RILEM Tech. Lett.* **2020**, *4*, 130–137. [CrossRef]
52. Ricker, M.; Zecherle, K.; Binde, J.; Haxter, C.; Winkelmann, J. Tensile Behavior of Concrete Components Reinforced with Natural-Fiber Textiles. *BFT International*. 8 2022. Available online: https://www.bft-international.com/en/artikel/bft_tensile_behavior_of_concrete_components_reinforced_with_natural-fiber-3816459.html (accessed on 15 June 2023).
53. Alan Strauss Rambo, D.; Umbinger de Oliveira, C.; Pícolo Salvador, R.; Dias Toledo Filho, R.; da Fonseca Martins Gomes, O.; de Andrade Silva, F.; de Melo Vieira, M. Sisal Textile Reinforced Concrete: Improving Tensile Strength and Bonding through Peeling and Nano-Silica Treatment. *Constr. Build. Mater.* **2021**, *301*, 124300. [CrossRef]
54. Fidelis, M.E.A.; de Andrade Silva, F.; Toledo Filho, R.D. The Influence of Fiber Treatment on the Mechanical Behavior of Jute Textile Reinforced Concrete. *Key Eng. Mater.* **2014**, *600*, 469–474. [CrossRef]
55. Ferrara, G.; Pepe, M.; Toledo Filho, R.D.; Martinelli, E. Mechanical Response and Analysis of Cracking Process in Hybrid TRM Composites with Flax Textile and Curauá Fibres. *Polymers* **2021**, *13*, 715. [CrossRef] [PubMed]
56. Majstorović, F.; Sebera, V.; Mrak, M.; Dolenec, S.; Wolf, M.; Marrot, L. Impact of Metakaolin on Mechanical Performance of Flax Textile-Reinforced Cement-Based Composites. *Cem. Concr. Compos.* **2022**, *126*, 104367. [CrossRef]

57. Hakamy, A.; Shaikh, F.U.A.; Low, I.M. Characteristics of Hemp Fabric Reinforced Nanoclay–Cement Nanocomposites. *Cem. Concr. Compos.* **2014**, *50*, 27–35. [CrossRef]
58. Li, D.; Ding, Y.; Wang, Q.; Zhang, Y.; Azevedo, C.; Zhang, Y. Hybrid Effect of Fibre Mesh and Short Fibres on the Biaxial Bending Behaviour of TRC. *Mag. Concr. Res.* **2019**, *71*, 869–880. [CrossRef]
59. Fischer, G.; Li, V. Influence of Matrix Ductility on Tension-Stiffening Behavior of Steel Reinforced Engineered Cementitious Composites (ECC). *ACI Struct. J.* **2002**, *99*, 11041. [CrossRef]
60. Barhum, R.; Mechtcherine, V. Effect of Short, Dispersed Glass and Carbon Fibres on the Behaviour of Textile-Reinforced Concrete under Tensile Loading. *Eng. Fract. Mech.* **2012**, *92*, 56–71. [CrossRef]
61. Ramakrishna, G.; Priyadharshini, S. Effect of Embedment Length of Untreated Natural Fibres on the Bond Behaviour in Cement Mortar. *Front. Struct. Civ. Eng.* **2018**, *12*, 454–460. [CrossRef]
62. Ferreira, S.R.; Martinelli, E.; Pepe, M.; de Andrade Silva, F.; Toledo Filho, R.D. Inverse Identification of the Bond Behavior for Jute Fibers in Cementitious Matrix. *Compos. Part B Eng.* **2016**, *95*, 440–452. [CrossRef]
63. Lima, P.R.L.; Santos, H.M.; Camilloto, G.P.; Cruz, R.S. Effect of Surface Biopolymeric Treatment on Sisal Fiber Properties and Fiber-Cement Bond. *J. Eng. Fibers Fabr.* **2017**, *12*, 155892501701200. [CrossRef]
64. Asprone, D.; Durante, M.; Prota, A.; Manfredi, G. Potential of Structural Pozzolanic Matrix–Hemp Fiber Grid Composites. *Constr. Build. Mater.* **2011**, *25*, 2867–2874. [CrossRef]
65. Rocha Ferreira, S.; Rodrigues Sena Neto, A.; De Andrade Silva, F.; Gomes De Souza, F.; Dias Toledo Filho, R. The Influence of Carboxylated Styrene Butadiene Rubber Coating on the Mechanical Performance of Vegetable Fibers and on Their Interface with a Cement Matrix. *Constr. Build. Mater.* **2020**, *262*, 120770. [CrossRef]
66. Peled, A.; Bentur, A.; Yankelevsky, D. Effects of Woven Fabric Geometry on the Bonding Performance of Cementitious Composites. *Adv. Cem. Based Mater.* **1998**, *7*, 20–27. [CrossRef]
67. Galzerano, B.; Formisano, A.; Durante, M.; Iucolano, F.; Caputo, D.; Liguori, B. Hemp Reinforcement in Lightweight Geopolymers. *J. Compos. Mater.* **2018**, *52*, 2313–2320. [CrossRef]
68. Ferreira, S.R.; Pepe, M.; Martinelli, E.; de Andrade Silva, F.; Toledo Filho, R.D. Influence of Natural Fibers Characteristics on the Interface Mechanics with Cement Based Matrices. *Compos. Part B Eng.* **2018**, *140*, 183–196. [CrossRef]
69. Abbass, A.; Lourenço, P.B.; Oliveira, D.V. The Use of Natural Fibers in Repairing and Strengthening of Cultural Heritage Buildings. *Mater. Today Proc.* **2020**, *31*, S321–S328. [CrossRef]
70. Mercedes, L.; Bernat-Maso, E.; Gil, L. In-Plane Cyclic Loading of Masonry Walls Strengthened by Vegetal-Fabric-Reinforced Cementitious Matrix (FRCM) Composites. *Eng. Struct.* **2020**, *221*, 111097. [CrossRef]
71. Cassese, P.; Balestrieri, C.; Fenu, L.; Asprone, D.; Parisi, F. In-Plane Shear Behaviour of Adobe Masonry Wallets Strengthened with Textile Reinforced Mortar. *Constr. Build. Mater.* **2021**, *306*, 124832. [CrossRef]
72. Gkournelos, P.D.; Azdejković, L.D.; Triantafillou, T.C. Innovative and Eco-Friendly Solutions for the Seismic Retrofitting of Natural Stone Masonry Walls with Textile Reinforced Mortar: In- and Out-of-Plane Behavior. *J. Compos. Constr.* **2022**, *26*, 04021061. [CrossRef]
73. Menna, C.; Asprone, D.; Durante, M.; Zinno, A.; Balsamo, A.; Prota, A. Structural Behaviour of Masonry Panels Strengthened with an Innovative Hemp Fibre Composite Grid. *Constr. Build. Mater.* **2015**, *100*, 111–121. [CrossRef]
74. Trochoutsou, N.; Di Benedetti, M.; Pilakoutas, K.; Guadagnini, M. In-Plane Cyclic Performance of Masonry Walls Retrofitted with Flax Textile–Reinforced Mortar Overlays. *J. Compos. Constr.* **2022**, *26*, 04022049. [CrossRef]
75. Cevallos, O.A.; Olivito, R.S.; Codispoti, R.; Ombres, L. Flax and Polyparaphenylene Benzobisoxazole Cementitious Composites for the Strengthening of Masonry Elements Subjected to Eccentric Loading. *Compos. Part B Eng.* **2015**, *71*, 82–95. [CrossRef]
76. de Carvalho Bello, C.B.; Baraldi, D.; Cecchi, A.; Oliveira, D.V. Experimental Characterization of Masonry Panels Strengthened with NFRCM. *Key Eng. Mater.* **2021**, *898*, 43–48. [CrossRef]
77. Trochoutsou, N.; Pilakoutas, K.; Guadagnini, M. FLAX-TRM for the In-Plane Shear Strengthening of Masonry. *Key Eng. Mater.* **2022**, *916*, 443–448. [CrossRef]
78. Trochoutsou, N.; Di Benedetti, M.; Pilakoutas, K.; Guadagnini, M. Bond of Flax Textile-Reinforced Mortars to Masonry. *Constr. Build. Mater.* **2021**, *284*, 122849. [CrossRef]
79. de Felice, G.; De Santis, S.; Garmendia, L.; Ghiassi, B.; Larrinaga, P.; Lourenço, P.B.; Oliveira, D.V.; Paolacci, F.; Papanicolaou, C.G. Mortar-Based Systems for Externally Bonded Strengthening of Masonry. *Mater. Struct.* **2014**, *47*, 2021–2037. [CrossRef]
80. De Santis, S.; de Felice, G.; Roscini, F. Retrofitting of Masonry Vaults by Basalt Textile-Reinforced Mortar Overlays. *Int. J. Archit. Herit.* **2019**, *13*, 1061–1077. [CrossRef]
81. Hojdys, Ł.; Krajewski, P. Tensile Behaviour of FRCM Composites for Strengthening of Masonry Structures—An Experimental Investigation. *Materials* **2021**, *14*, 3626. [CrossRef] [PubMed]
82. Lignola, G.P.; Caggegi, C.; Ceroni, F.; De Santis, S.; Krajewski, P.; Lourenço, P.B.; Morganti, M.; Papanicolaou, C.; Pellegrino, C.; Prota, A.; et al. Performance Assessment of Basalt FRCM for Retrofit Applications on Masonry. *Compos. Part B Eng.* **2017**, *128*, 1–18. [CrossRef]
83. Ascione, L.; de Felice, G.; De Santis, S. A Qualification Method for Externally Bonded Fibre Reinforced Cementitious Matrix (FRCM) Strengthening Systems. *Compos. Part B Eng.* **2015**, *78*, 497–506. [CrossRef]
84. Larrinaga, P.; Chastre, C.; Biscaia, H.C.; San-José, J.T. Experimental and Numerical Modeling of Basalt Textile Reinforced Mortar Behavior under Uniaxial Tensile Stress. *Mater. Des.* **2014**, *55*, 66–74. [CrossRef]

85. Dalalbashi, A.; Ghiassi, B.; Oliveira, D.V. A Multi-Level Investigation on the Mechanical Response of TRM-Strengthened Masonry. *Mater. Struct.* **2021**, *54*, 224. [CrossRef]
86. De Santis, S.; de Felice, G. Steel Reinforced Grout Systems for the Strengthening of Masonry Structures. *Compos. Struct.* **2015**, *134*, 533–548. [CrossRef]
87. Arboleda, D.; Carozzi, F.G.; Nanni, A.; Poggi, C. Testing Procedures for the Uniaxial Tensile Characterization of Fabric-Reinforced Cementitious Matrix Composites. *J. Compos. Constr.* **2016**, *20*, 04015063. [CrossRef]
88. De Santis, S.; Hadad, H.A.; De Caso y Basalo, F.; de Felice, G.; Nanni, A. Acceptance Criteria for Tensile Characterization of Fabric-Reinforced Cementitious Matrix Systems for Concrete and Masonry Repair. *J. Compos. Constr.* **2018**, *22*, 04018048. [CrossRef]
89. Caggegi, C.; Carozzi, F.G.; De Santis, S.; Fabbrocino, F.; Focacci, F.; Hojdys, Ł.; Lanoye, E.; Zuccarino, L. Experimental Analysis on Tensile and Bond Properties of PBO and Aramid Fabric Reinforced Cementitious Matrix for Strengthening Masonry Structures. *Compos. Part B Eng.* **2017**, *127*, 175–195. [CrossRef]
90. Carozzi, F.G.; Bellini, A.; D'Antino, T.; de Felice, G.; Focacci, F.; Hojdys, Ł.; Laghi, L.; Lanoye, E.; Micelli, F.; Panizza, M.; et al. Experimental Investigation of Tensile and Bond Properties of Carbon-FRCM Composites for Strengthening Masonry Elements. *Compos. Part B Eng.* **2017**, *128*, 100–119. [CrossRef]
91. De Santis, S.; de Felice, G. Tensile Behaviour of Mortar-Based Composites for Externally Bonded Reinforcement Systems. *Compos. Part B Eng.* **2015**, *68*, 401–413. [CrossRef]
92. Hegger, J.; Will, N.; Bruckermann, O.; Voss, S. Load–Bearing Behaviour and Simulation of Textile Reinforced Concrete. *Mater. Struct.* **2006**, *39*, 765–776. [CrossRef]
93. Carozzi, F.G.; Poggi, C. Mechanical Properties and Debonding Strength of Fabric Reinforced Cementitious Matrix (FRCM) Systems for Masonry Strengthening. *Compos. Part B Eng.* **2015**, *70*, 215–230. [CrossRef]
94. Bertolesi, E.; Carozzi, F.G.; Milani, G.; Poggi, C. Numerical Modeling of Fabric Reinforce Cementitious Matrix Composites (FRCM) in Tension. *Constr. Build. Mater.* **2014**, *70*, 531–548. [CrossRef]
95. Saidi, M.; Gabor, A. Iterative Analytical Modelling of the Global Behaviour of Textile-Reinforced Cementitious Matrix Composites Subjected to Tensile Loading. *Constr. Build. Mater.* **2020**, *263*, 120130. [CrossRef]
96. Enrico Garbin, M.P. Maria Rosa Valluzzi Experimental Characterization of Glass and Carbon FRCMs for Masonry Retrofitting. *ACI Symp. Publ.* **2018**, *324*, 3.1–3.20. [CrossRef]
97. Rampini, M.C.; Zani, G.; Colombo, M.; di Prisco, M. Mechanical Behaviour of TRC Composites: Experimental and Analytical Approaches. *Appl. Sci.* **2019**, *9*, 1492. [CrossRef]
98. Valeri, P.; Fernàndez Ruiz, M.; Muttoni, A. Tensile Response of Textile Reinforced Concrete. *Constr. Build. Mater.* **2020**, *258*, 119517. [CrossRef]
99. De Santis, S.; Ceroni, F.; de Felice, G.; Fagone, M.; Ghiassi, B.; Kwiecień, A.; Lignola, G.P.; Morganti, M.; Santandrea, M.; Valluzzi, M.R.; et al. Round Robin Test on Tensile and Bond Behaviour of Steel Reinforced Grout Systems. *Compos. Part B Eng.* **2017**, *127*, 100–120. [CrossRef]
100. Donnini, J.; Corinaldesi, V. Mechanical Characterization of Different FRCM Systems for Structural Reinforcement. *Constr. Build. Mater.* **2017**, *145*, 565–575. [CrossRef]
101. Donnini, J.; De Caso y Basalo, F.; Corinaldesi, V.; Lancioni, G.; Nanni, A. Fabric-Reinforced Cementitious Matrix Behavior at High-Temperature: Experimental and Numerical Results. *Compos. Part B Eng.* **2017**, *108*, 108–121. [CrossRef]
102. Jahangir, H.; Esfahani, M.R. Experimental Analysis on Tensile Strengthening Properties of Steel and Glass Fiber Reinforced Inorganic Matrix Composites. *Sci. Iran.* **2021**, *28*, 1152–1166. [CrossRef]
103. Morales Cruz, C.; Raupach, M. Influence of the Surface Modification by Sanding of Carbon Textile Reinforcements on the Bond and Load-Bearing Behavior of Textile Reinforced Concrete. *MATEC Web Conf.* **2019**, *289*, 04006. [CrossRef]
104. Bellini, A.; Aiello, M.A.; Bencardino, F.; De Carvalho Bello, C.B.; Castori, G.; Cecchi, A.; Ceroni, F.; Corradi, M.; D'Antino, T.; De Santis, S.; et al. Influence of Different Set-up Parameters on the Bond Behavior of FRCM Composites. *Constr. Build. Mater.* **2021**, *308*, 124964. [CrossRef]
105. D'Ambrisi, A.; Focacci, F. Flexural Strengthening of RC Beams with Cement-Based Composites. *J. Compos. Constr.* **2011**, *15*, 707–720. [CrossRef]
106. Elsanadedy, H.M.; Almusallam, T.H.; Alsayed, S.H.; Al-Salloum, Y.A. Flexural Strengthening of RC Beams Using Textile Reinforced Mortar—Experimental and Numerical Study. *Compos. Struct.* **2013**, *97*, 40–55. [CrossRef]
107. Mercedes, L.; Mendizábal, V.; Bernat-Maso, E.; Gil, L. Performance of Hemp-FRCM-Strengthened Beam Subjected to Cyclic Loads. *Mater. Constr.* **2022**, *72*, e270. [CrossRef]
108. Aveston, J.; Cooper, G.A.; Kelly, A. Single and Multiple Fracture. In *Proceedings of the National Physical Laboratory Conference: The Properties of Fiber Composites*; IPC Science and Technology Press Ltd.: Guildford, UK, 1971; pp. 15–26.
109. Mallick, P.K. *Fiber-Reinforced Composites: Materials, Manufacturing, and Design*, 3rd ed.; CRC Press: Boca Raton, FL, USA, 2007; ISBN 978-0-429-12206-4.
110. Mansor, M.R.; Sapuan, S.M.; Zainudin, E.S.; Nuraini, A.A.; Hambali, A. Stiffness Prediction of Hybrid Kenaf/Glass Fiber Reinforced Polypropylene Composites Using Rule of Mixtures (ROM) and Rule of Hybrid Mixtures (RoHM). *J. Polym. Mater.* **2013**, *30*, 321–334.

111. Kelly, A. Fracture Phenomena in Composites. In Proceedings of the International Conference on Fracture ICF3, Munich, Germany, 14 October 1973.
112. Aveston, J.; Kelly, A. Theory of Multiple Fracture of Fibrous Composites. *J. Mater. Sci.* **1973**, *8*, 352–362. [CrossRef]
113. Kimber, A.C.; Keer, J.G. On the Theoretical Average Crack Spacing in Brittle Matrix Composites Containing Continuous Aligned Fibres. *J. Mater. Sci. Lett.* **1982**, *1*, 353–354. [CrossRef]
114. Curtin, W.A. Stochastic Damage Evolution and Failure in Fiber-Reinforced Composites. In *Advances in Applied Mechanics*; Elsevier: Amsterdam, The Netherlands, 1998; Volume 36, pp. 163–253. ISBN 978-0-12-002036-2.
115. Fédération Internationale du béton (fib). *fib Model Code for Concrete Structures 2010—MC2010*; Fédération Internationale du Béton: Lausanne, Switzerland, 2013.
116. *EN 1992-1-1*; Eurocode 2: Design of Concrete Structures: General Rules and Rules for Buildings. CEN: Brussels, Belgium, 2004.
117. Li, V.C.; Wu, H.-C. Conditions for Pseudo Strain-Hardening in Fiber Reinforced Brittle Matrix Composites. *Appl. Mech. Rev.* **1992**, *45*, 390–398. [CrossRef]